Global Advanced Research Journal of Agricultural Science (ISSN: 2315-5094) Vol. 4(4) pp. 200-210, April, 2015.
Available online http://garj.org/garjas/index.htm

Full Length Research Paper

Nonlinear mixed-effects models for the modeling the effects of growth rate on the transition of juvenile to mature wood in basic density in hinoki cypress (*Chamaecyparis obtusa*)

Takaaki Fujimoto *[1] And [2]Junji Kimura

[1]Faculty of Agriculture, Tottori University, Tottori, 680-8553, Japan
TEL&FAX: +81-857-31-5866
[2]Tohoku Regional Forest Office, Forestry Agency, Akita, 010-8550, Japan
TEL&FAX: +81-18-836-2014

Accepted 16 March, 2015

The aim of this study was to evaluate the effects of growth rate on the radial variation in basic density of hinoki cypress (*Chamaecyparis obtusa*) using a nonlinear mixed-effects model. Nineteen sample trees were harvested from two plots in which trees showed different growth rates within a 50-year-old hinoki stand. Ring widths and basic density were measured at 5-ring intervals. An asymptotic regression model that included the random effects of individual trees was fitted to describe the radial variation in basic density. A model including the fixed-effects of the plots as the covariate was also tested. The results indicated that the terms of the plots were highly significant; thus, the growth rate would affect the radial variation in basic density. The transition age was defined as the ring at which the basic density reached approximately 99% of the asymptote. The transition ages varied among trees, and ranged from 13.0 to 26.0. Analysis of variance revealed that the transition ages of trees in fast-growth plots were significantly younger than those of trees in slow-growth plots. These results imply that fast growth may be related to an early age of transition from juvenile to mature wood.

Keywords: Growth rate; Transition from juvenile to mature wood; Nonlinear mixed-effect model; *Chamaecyparis obtusa*

INTRODUCTION

Hinoki cypress (*Chamaecyparis obtusa*) has been grown intensively since the middle of last century. At present, the forest area of hinoki cypress accounts for approximately 25% of all plantation areas in Japan (Forestry Agency, 2013). Since hinoki cypress shows remarkable mechanical properties and durability (Forests and Forestry Products Research Institute, 1982), it has been used to produce high-quality building materials. However, the reputation of hinoki has gradually decreased as the resources have shifted from natural to plantation forests. There are few reports on the wood properties of hinoki from plantation forests. Accurate analyses of the wood properties of the currently available hinoki resources are necessary for appropriate forest management and utilization.

Wood uniformity is a very important attribute for the final wood product (Zobel and Sprague, 1998). As stated by Zobel and Buijtenen (1989), the main cause of wood variation is the presence of juvenile wood, and its proportion relative to that of mature wood. In general, juvenile wood is less suitable than mature wood for use in solid wood products. This is because juvenile wood is characterized by shorter cells, larger microfibril angles, weaker mechanical properties, and lower dimensional stability than mature wood. Thus, the proportion of juvenile wood in logs strongly affects the quality of forest resources.

The effect of growth rate on the age of the transition from juvenile to mature wood has been investigated in a number of studies, but the results have been controversial. Loo *et al*. (1985) reported that a high growth rate was negatively correlated with transition age in loblolly pine. Shiokura and Kobayashi (1984) reported similar results for sugi (*Cryptomeria japonica*), but they pointed out that the radius of the juvenile wood area increased with growth rate. Zobel *et al*. (1959) reported the opposite results for loblolly and slash pines; that is, the juvenile period in trees in rapidly growing plantations at better sites or at fertilized sites was the same as, or longer than, that of trees growing at poor sites. There was no clear relationship between growth rate and transition age in Douglas fir (Abdel-Gadir and Krahmer, 1993; Vargas-Hernandez *et al*., 1994).

In a previous study (Kimura and Fujimoto, 2014), the effects of growth rate on the intra-tree variation in basic density in 50-year-old hinoki were examined using a linear mixed-effects (LME) model. Although the model with a quadratic function for cambial age described the intra-tree variation well, it would be inadequate for predictions beyond the observed range of the data. Recently, a nonlinear mixed-effects (NLME) model has been applied to evaluate variations in various wood properties (Jordan *et al*., 2005; Schneider *et al*., 2008). For instance, such models have been used to evaluate the transition from juvenile wood to mature wood (Mutz *et al*., 2004; Mora *et al*., 2007). Because nonlinear models are based on a model for the mechanism producing the response, the parameters in a nonlinear model generally have a natural physical interpretation (Pinheiro and Bates, 2000). A nonlinear model generally gives a more parsimonious description of the data, and also provides reliable predictions for the response variable even outside the observed range of the data.

The objective of this study was to fit a descriptive model to the radial variation in basic density of hinoki cypress using a nonlinear mixed-effects model. Based on this model, the transition age from juvenile to mature wood was estimated, and the effects of growth rate on the transition age were evaluated.

Sample origin and preparation

Sample materials were obtained from 50-year-old Hinoki cypress stands in Tottori University Forest located in

*Corresponding Author's E-mail: tafujimoto@muses.tottori-u.ac.jp; TEL&FAX: +81-857-31-5866

Maniwa, Okayama (35°16' N, 133°36' E; approximately 540 m elevation), Japan. This stand has been described in detail in a previous article (Kimura and Fujimoto, 2014). The test stand consisted of four 10-m square plots; two fast-growth plots and two slow-growth plots. Details of the test stand are summarized in Table 1. Although the detailed history of the stand is unclear, the fast-growth plots had been thinned several times, whereas the slow-growth plots had never been thinned previously. As a result, the stand density differed between the fast- and slow-growth plots. Four or five trees were felled from each plot (in total, 19 trees) in 2012. The height, diameter at breast height (DBH), and height to the base of live crown (BLC) were measured at harvest (Table 1). Analysis of variance confirmed significant differences in DBH among plots ($p = 0.006$; data not shown).

Disks were cut from sample trees at heights of 2 and 4 m, and then at 4-m intervals to the 16-m position. In this study, we used the disks at a single height position for analyses. Since the proportion of juvenile wood varies with height position, it is appropriate to consider relative height when collecting sample disks, i.e., height position divided by total tree height. The mean values of the relative height at the 2-m position on trees in plot A1, A2, B1, and B2 were 0.11, 0.11, 0.12, and 0.18, respectively, and those at the 4-m position were 0.23, 0.23, 0.23, and 0.35, respectively. Hence, we used the disks from the 4-m position from trees in Plots A1, A2, and B1, and from the 2-m position from trees in plot B2. The radius of the sample disks is shown in Table 1. Radial strips were cut from the disks and ring width was measured every five rings from the pith outwards. Measurements were taken in two radial directions and ring width was expressed as the mean of both values to represent the average trends in the sample disks. Then, the strips were cut into 5-ring portions for basic density analysis. The water displacement method was used to determine basic density. Basic density was determined as the mean value from both radial directions. Radial variations in basic density and the radius of the sample disks from trees in each plot are shown in Figure 1.

Model development

A NLME model was used to describe the radial variation in basic density shown in Figure1. The nlme package (Pinheiro *et al*., 2013) in R version 3.0.0 was used to fit models. The NLME model requires starting estimates for the fixed-effects coefficients (Pinheiro and Bates, 2000). The nlme library includes several self-starting model functions that can be used to fit nonlinear regression models in R without specifying starting estimates for the parameters. As the start model (model-1), we selected the following asymptotic regression:

$$BD_{ij} = \phi_{1i} + (\phi_{2i} - \phi_{1i})\exp\left[-\exp(\phi_{3i})AGE_j\right] + \varepsilon_{ij}, \quad \varepsilon_{ij} \sim N(0, \sigma^2), \tag{1}$$

where BD_{ij} is the basic density of the jth age in the ith tree, AGE is the cambial age, ϕ_{1i} is the asymptote as $AGE \to \infty$, ϕ_{2i} is the initial value of BD, ϕ_{3i} is the natural logarithm of the rate constant, and ε_{ij} is the within-group error, which is assumed to be independent for different i and j normally distributed with mean 0 and variance σ^2. The parameter vector ϕ_i was modeled as follows:

$$\boldsymbol{\varphi}_i = \begin{bmatrix} \phi_{1i} \\ \phi_{2i} \\ \phi_{3i} \end{bmatrix} = \begin{bmatrix} \beta_1 \\ \beta_2 \\ \beta_3 \end{bmatrix} + \begin{bmatrix} b_{1i} \\ b_{2i} \\ b_{3i} \end{bmatrix} = \boldsymbol{\beta} + \boldsymbol{b}_i, \quad \boldsymbol{b}_i \sim N(0, \boldsymbol{\Psi}), \tag{2}$$

where $\boldsymbol{\beta} = (\beta_1, \beta_2, \beta_3)^T$ is the fixed effect representing the population mean of the individual parameters $\boldsymbol{\phi}_i$, and $\boldsymbol{b}_i = (b_{1i}, b_{2i}, b_{3i})^T$ is the random effect of the ith tree. The random effects $\boldsymbol{b}_i$ are assumed to be independent for different trees. The variance-covariance matrix $\boldsymbol{\Psi}$ is set to be diagonal. All of the model parameters in this article were estimated by the maximum likelihood method.

To determine the fixed-effects structure, the initial test was

Table 1.Characteristics of plots and sample trees in the test stand*

		Plot A (thinned)		Plot B (unthinned)	
		A1	A2	B1	B2
Stand density	(tree/ha)	1000	1200	2100	2800
BA	(m^2/ha)	50.9	52.5	63.2	42.0
DBH	(cm)	22.8 (19.0–26.3)	26.9 (23.9–30.9)	19.9 (18.8–21.2)	13.6 (11.9–16.0)
Height	(m)	17.6 (17.1–18.3)	17.5 (16.4–18.6)	17.2 (15.2–18.3)	11.5 (10.2–12.7)
BLC	(m)	11.2 (10.5–11.8)	9.1 (7.7–9.9)	11.1 (7.4–13.1)	5.5 (4.2–7.1)
RAD	(cm)	9.6 (7.3–11.3)	11.4 (9.6–15.0)	8.1 (7.0–9.7)	5.9 (4.9–7.2)

BA: basal area; DBH: diameter at breast height; BLC: height to the base of live crown; RAD: radius of sample disks.

*Data were obtained when sample trees were harvested. DBH, Height, BLC, and RAD are the mean values of sample trees. Values in parentheses indicate range (minimum to maximum).

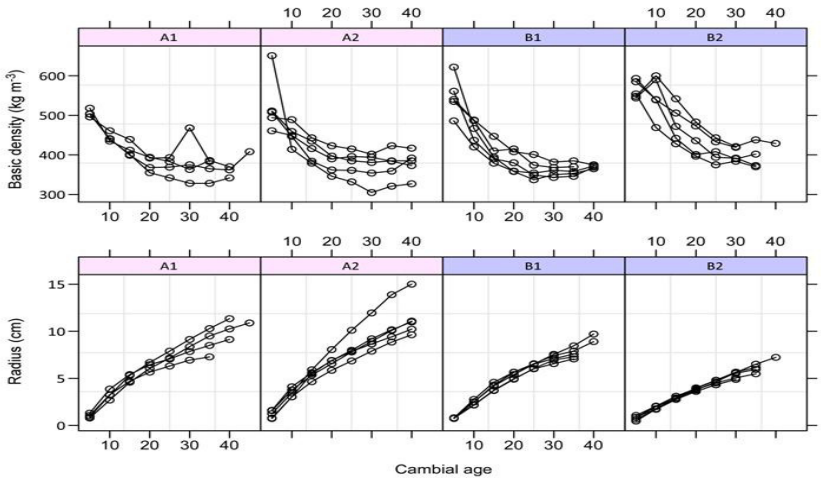

Figure1. Radial variation in basic density and radius of sample disks from trees in fast-growth plots (A1 and A2) and slow-growth plots (B1 and B2).

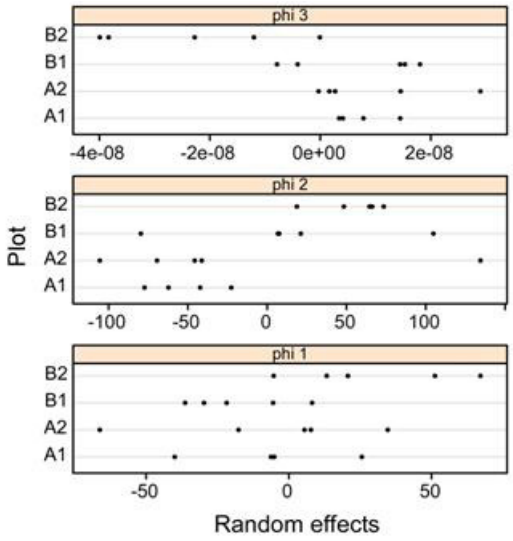

Figure 2. Dotplots of estimated random effects corresponding to model-1 versus all growth plots.

whether the growth rate significantly affected the radial variation in basic density. It should be noted that embedding covariates in the model to explain intergroup variation generally reduces the number of random effects in the model, and leads to a better understanding of the mechanism producing the response (Pinheiro and Bates, 2000). Dotplots of estimated random effects corresponding to model-1 versus all growth plots are shown in Figure 2. There were moderate relationships between the covariates and all parameters in eq. (1). For instance, the log-rate parameters ϕ_{3i} were higher for the fast-growth plots than for the slow-growth plots. Thus, the next model (model-2) included the fixed-effects of the plots as the covariate.

$$\boldsymbol{\varphi}_i = \begin{bmatrix} \phi_{1i} \\ \phi_{2i} \\ \phi_{3i} \end{bmatrix} = \begin{bmatrix} \beta_1 + \gamma_{12}x_{2i} + \gamma_{13}x_{3i} + \gamma_{14}x_{4i} \\ \beta_2 + \gamma_{22}x_{2i} + \gamma_{23}x_{3i} + \gamma_{24}x_{4i} \\ \beta_3 + \gamma_{32}x_{2i} + \gamma_{33}x_{3i} + \gamma_{34}x_{4i} \end{bmatrix} + \begin{bmatrix} b_{1i} \\ b_{2i} \\ b_{3i} \end{bmatrix}, \quad (3)$$

where x_{2i} is a binary variable taking the value 1 if the ith tree grew in Plot A2; x_{3i} and x_{4i} are the binary indicator variables for Plots B1 and B2, respectively; β_1, β_2, and β_3 are the average asymptote, initial value, and log-rate, respectively, for Plot A1; and γ_{1k}, γ_{2k}, and γ_{3k} are the kth plot effects associated with the coefficients $\boldsymbol{\phi}_i$. We tested the joint significance of the fixed-effects included in model-2. The results revealed that the terms of the plots were highly significant ($p<$ 0.0001). Model-1 and model-2 were compared using the log-likelihood ratio test (LRT), the Akaike's information criterion (AIC), and the Schwarz's Bayesian information criterion (BIC). The p-value ($p<$ 0.0001) for the LRT and the smaller AIC and BIC values (data not shown) for model-2 indicated that the inclusion of the plot effects clearly improved the performance of the model. These results implied that the growth rate would affect the radial variation in the basic density of hinoki.

As mentioned above, the variance-covariance matrix $\boldsymbol{\Psi}$in model-2 was set to be diagonal. Although the structure of the general positive definite was also tested, the calculations could not reach convergence. Consequently, no further modifications were made to the variance–covariance structure of random effects.

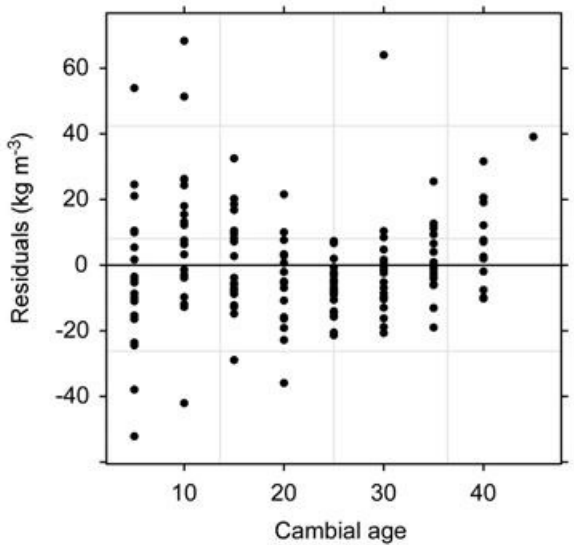

Figure 3. Plot of residuals versus cambial age for model-2 with homoscedastic within-group errors.

Table 2. Performance of models with different within-group error variance structures

Model	Variance function	No. of parameters	AIC	BIC	LogLik	LRT	*p*-value
2	No structure	16	1396	1443	-681.8		
2.1	Power	17	1355	1406	-660.6	42.5	<0.0001
2.2	Exponential	17	1354	1405	-660.1	43.5	<0.0001
2.3	ConstPower	18	1357	1410	-660.1	42.5	<0.0001

AIC: Akaike's information criterion; BIC: Schwarz's Bayesian information criterion; LogLik: log-likelihood estimated by maximum likelihood method; LRT: likelihood ratio test calculated with respect to model-2

The within-group error, ε_{ij}, was assumed to be independent for different *i* and *j* and independent of the random effects in model-2. The plots of residuals versus cambial age (*AGE*) indicated that the residuals slightly decreased with *AGE* (Figure 3). Thus, the variance structure of the within-group error was specified to account for heteroscedasticity. Variance functions are used to model the variance structure of within-group errors using covariates (Davidian and Giltinan, 1995; Pinheiro and Bates, 2000). In this case, the cambial age is a natural candidate for the variance covariate. The variance functions included in the nlme package (i.e., power, exponential, and constant plus power of covariance models) were tested. There were significant increases in the log-likelihood, as evidenced by the large LRT value, indicating that addition of the variance function to the model significantly improved model-2 (Table 2). Based on AIC and BIC, the exponential function of age

(model-2.2) was the best candidate variance structure of within-group error.

Since the age trend of basic density could be considered as time-series data, temporal autocorrelations should be taken into account. Serial correlation structures are used to model dependence in time-series data (Box *et al*., 1994). The empirical autocorrelation at lag *l* ($\hat{\rho}(l)$) for model-2.2 residuals was calculated as follows:

$$\begin{aligned}\hat{\rho}(l) &= \left[\hat{\rho}(1),\ \hat{\rho}(2),\ \hat{\rho}(3),\ \hat{\rho}(4),\ \hat{\rho}(5)\right]^{\mathrm{T}} \\ &= \left[-0.098,\ -0.187,\ -0.151,\ -0.119,\ -0.325\right]^{\mathrm{T}}.\end{aligned} \quad (4)$$

No significant autocorrelations were found in model-2.2. Several serial correlation structures were tested (e.g., autoregressive and moving average correlation models) but they could not improve model-2.2 (data not shown). Hence, the following model was finally obtained to describe the radial variation in basic density.

$$\begin{aligned} BD_{ij} &= \phi_{1i} + (\phi_{2i} - \phi_{1i})\exp\left[-\exp(\phi_{3i})AGE_j\right] + \varepsilon_{ij}\ , \\ \boldsymbol{\varphi}_i &= \begin{bmatrix}\phi_{1i}\\ \phi_{2i}\\ \phi_{3i}\end{bmatrix} = \begin{bmatrix}\beta_1 + \gamma_{12}x_{2i} + \gamma_{13}x_{3i} + \gamma_{14}x_{4i}\\ \beta_2 + \gamma_{22}x_{2i} + \gamma_{23}x_{3i} + \gamma_{24}x_{4i}\\ \beta_3 + \gamma_{32}x_{2i} + \gamma_{33}x_{3i} + \gamma_{34}x_{4i}\end{bmatrix} + \begin{bmatrix}b_{1i}\\ b_{2i}\\ b_{3i}\end{bmatrix}, \\ \boldsymbol{b}_i &\sim N\left(0, \begin{pmatrix}\sigma_{11} & 0 & 0\\ 0 & \sigma_{22} & 0\\ 0 & 0 & \sigma_{33}\end{pmatrix}\right),\ \ \varepsilon_{ij} \sim N\left(0,\ \sigma^2 G_{ij}^{\gamma/2}(\upsilon_{ij},\ \delta) C_{ij}\, G_{ij}^{\gamma/2}(\upsilon_{ij},\ \delta)\right), \end{aligned} \quad (5)$$

Where G_{ij} is the variance function with a vector of variance covariate υ_{ij} and a vector of variance parameters δ; and C_{ij} is the correlation of within-group errors ε_{ij}. The remaining elements of the model have been described previously. The structure of G_{ij} is calculated as follows:

$$G(\upsilon_{ij},\ \delta) = \exp(\delta\upsilon_{ij}). \quad (6)$$

The C_{ij} does not have a specific correlation structure. Parameter estimates and corresponding standard errors for fixed effects of the final model [Eq. (5)] are shown in Table 3. The augmented predictions (Pinheiro and Bates, 2000) for each tree were plotted to assess the adequacy of the final model (Figure 4). The plots include the observed values of basic density (open circles), predictions based on estimated fixed-effects parameters of the final model excluding random effects (solid lines), and predictions based on the final model including random effects (dashed lines). The predictions from the model including the random effects followed the observed values closely, indicating that the final model explained the density variation data well.

Transition from juvenile to mature wood

As defined by Zobel and Sprague (1998), the juvenile wood zone is the area of rapid changes in properties near the pith, whereas the mature wood with more uniform properties is toward the bark. Several methods have been suggested to determine the age of the transition from juvenile to mature wood (Shiokura, 1982; Loo *et al*., 1985; Hodge and Purnell, 1993; Fujimoto *et al*., 2005; Mora *et al*., 2007). In this study, we defined the transition age as the ring at which the basic density reaches approximately 99% of the asymptote ϕ_{1i}. The estimated transition ages for each plot based on the final model are summarized in Table 4. The transition ages varied among trees, and ranged from 13.0 to 26.0. Analysis of variance revealed that the transition age of trees in Plots A1, A2, and B1 was significantly different from that of trees in Plot B2. These results implied that fast growth may be related to an early age of the transition from juvenile to mature wood.

DISCUSSIONS

In this study, a NLME model was applied to describe the radial variation in basic density in hinoki cypress. A model including the fixed-effects of the plots as the covariate was tested, to assess the effects of growth rate on the variation in basic density. The results indicated that the terms of the plots were highly significant, and thus, the growth rate would

Table 3.Estimated fixed-effects parameters of basic density

Parameters	Estimate	Std. error
Plot A1		
β_1	369.005	13.095
β_2	665.393	60.003
β_3	-1.955	0.188
Plot A2		
γ_{12}	370.577	17.484
γ_{22}	748.682	92.673
γ_{32}	-1.836	0.243
Plot B1		
γ_{13}	361.405	17.493
γ_{23}	820.645	102.586
γ_{33}	-1.823	0.236
Plot B2		
γ_{14}	383.848	20.255
γ_{24}	766.577	92.864
γ_{34}	-2.307	0.280

β_1 and γ_{1k} are the asymptote parameters for each plot; γ_2 and β_{2k} are the initial values of basic density; γ_3 and β_{3k} are the natural logarithms of the rate constant.

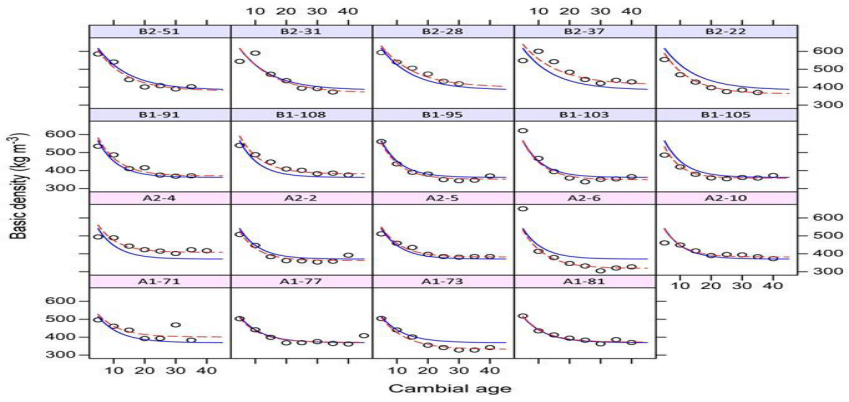

Figure 4. Population prediction (setting all random effects to 0), subject-specified predictions (including random effects) from the final model, and observed values of basic density versus cambial age. Solid blue lines, dotted red lines, and open circles show population predictions, subject-specified predictions, and observed values, respectively.

Table 4. Estimated transition age from juvenile to mature wood

	Transition age			Variance
Plot	Mean	Min	Max	Test
A1	15.2	13.0	19.0	a
A2	15.2	14.0	19.0	a
B1	16.2	14.0	17.0	a
B2	23.6	21.0	26.0	b

a and b indicate statistically significant (p< 0.0001) differences in transition age among plots

affect the radial variation in basic density. This result is inconsistent with those of our previous study (Kimura and Fujimoto, 2014); that is, the LME model consisting of a second-order polynomial function of cambial age did not show a significant effect of growth rate on the variation in basic density within the stem. Although the reason for this contradiction is unclear, the results may be affected by the methods of parameterization. The parameters in a NLME model, such as asymptotes and monotonicity, generally have a natural physical interpretation (Pinheiro and Bates, 2000). As shown in Figure 2, there were large differences among the plots in the parameters of asymptote ϕ_1 and initial value ϕ_2. The differences in initial value would be due to inherent abilities, but the asymptote, i.e., the basic density in mature wood, might be affected by the growth rate. It is generally difficult to obtain these interpretations from a LME model.

Because the random effects are unobserved quantities, maximum likelihood estimation in mixed-effects models involve the multiple integration for the conditional density of the data given the random effects with respect to the marginal density of the random effects (Pinheiro and Bates, 2000). Moreover, the marginal likelihood function for the NLME model does not have a closed-form expression. Thus, an approximate likelihood function must be used to estimate parameters. As a consequence, it is often difficult to obtain the solution of the likelihood function with increase of parameters. In this study, the calculation did not converge when the variance-covariance matrix had a general positive definite structure. Applications of Bayesian statistics with Markov chain Monte Carlo methods would be useful to estimate parameters in complicated models.

The transition age from juvenile to mature wood was negatively correlated with the growth rate in hinoki. This result agrees with those of previous studies on loblolly pine (Loo *et al*., 1985) and black spruce (Yang, 1994). It is incorrect to conclude that a fast-growing tree would have less juvenile wood, because the proportion of juvenile wood within the trunk should also be affected by growth rate. We could not estimate the proportion of juvenile wood, since a radial growth model was not developed in this study. However, based on the radius data of sample disks shown in Figure 1, the proportion of juvenile wood would be larger in slow-growth plots than in fast-growth plots. That is, the radius of the juvenile wood zone in trees in Plot A1, A2, B1, and B2 would be approximately 5 cm, 5 cm, 4–5 cm, and

4–5 cm, respectively. The proportion of juvenile wood could be estimated as the ratio of the radius of juvenile wood to the disk radius. The proportion of juvenile wood in trees in Plot A1, A2, B1, and B2 would be approximately 52%, 44%, 49%–62%, and 68%–85%, respectively. Hence, slow growth, e.g., due to a delay in thinning, could produce logs with a higher proportion of juvenile wood. In this study, the transition age was arbitrarily defined as the ring at which the basic density reached approximately 99% of the asymptote. Since the area of juvenile wood will vary depending on the definition of the transition age, a more objective method to define the transition is required for further research.

ACKNOWLEDGMENTS

The authors are grateful to Dr. Keisuke Kawakami of Tottori Prefectural Agriculture and Forest Research Institute for preparing the test specimens. We also thank Mr. Shogo Fukutomi and Ms. Asami Yoneda of Tottori University Forest for harvesting the sample trees.

REFERENCES

Abdel-Gadir AY, Krahmer RL (1993).Estimating the age of demarcation of juvenile and mature wood in Douglas-fir. Wood Fiber Sci. 25: 242–249.

Box GEP, Jenkins GM, Reinsel GC (1994). Time series analysis: Forecasting and control. 4th ed., John Wiley and Sons, Inc., Hoboken, New Jersey.

Davidian M, Giltinan DM (1995). Nonlinear models for repeated measurement data. Chapman and Hall, London, UK.

Forestry Agency (2013).Annual report on trends in forests and forestry, fiscal year 2012 (summary). http://www.rinya.maff.go.jp/j/kikaku/hakusyo/24hakusyo/pdf/h24summary.pdf. Accessed 22 Aug 2014.

Forests and Forestry Products Research Institute (FFPRI) (1982). Wood technology and wood utilization division: properties of important Japanese woods table of the properties of woods (Research note). Bull. For.& For. Res. Inst. 319:85–126.

Fujimoto T, Akutsu H, Kita K, Uchiyama K, Kuromaru M, Oda K (2005).Genetic variation in the age of transition from juvenile to mature wood in hybrid larch (*Larixgmelinii* var. *japonica*×*L. kaempferi*) F_1.MokuzaiGakkaishi 51:85–91.

Hodge GR, Purnell RC (1993). Genetic parameter estimates for wood density, transition age, and radial growth in slash pine. Can J For Res 23:1881–1891.

Jordan L, Daniels RF, Clark III A, He R (2005). Multilevel nonlinear mixed-effects models for the modeling of earlywood and latewood microfibril angle. For. Sci. 51:357–371.

Kimura J, Fujimoto T (2014). Modeling the effects of growth rate on the intra-tree variation in basic density in hinoki cypress (*Chamaecyparis obtusa*).J. Wood Sci. 60: 305-312.

Loo JA, Tauer CG, Mc New RW (1985).Genetic variation in the time of transition from juvenile to mature wood in loblolly pine (*Pinustaeda* L.).Silvae Genet. 34: 14–19.

Mora CR, Allen HL, Daniels RF, Clark A (2007). Modeling corewood–outerwood transition in loblolly pine using wood specific gravity. Can. J. For. Res. 37:999–1011.

Mutz R, Guilley E, Sauter UH, Nepveu G (2004). Modelling juvenile-mature wood transition in Scots pine (*Pinussylvestris* L.) using nonlinear mixed-effects models. Ann. For. Sci. 61:831–841.

Pinheiro J, Bates D, DebRoy S, Sarkar D (2013). nlme: Linear and nonlinear mixed effects models. R package, version 3.1-111.

Pinheiro JC, Bates DM (2000).Mixed-effects models in S and S-PLUS.Springer, New York.

Schneider R, Zhang SY, Swift DE, Bégin J, Lussier JM (2008).Predicting selected wood properties of jack pine following commercial thinning. Can. J. For. Res. 38:2030–2043.

Shiokura T (1982).Extent and differentiation of the juvenile wood zone in coniferous tree trunks.MokuzaiGakkaishi 28:85–90.

Shiokura T, Kobayashi J (1984).Studies on juvenile wood.Part 6.Extent by the early growth hastening of the juvenile wood zone in the tree trunks of SUGI (*Cryptomeria japonica* D. Don.). Journal of agriculture science, Tokyo NogyoDaigaku 29(1):18–22.

Vargas-Hernandez J, Adams WT, Krahmer RL (1994). Family variation in age trends of wood density traits in young coastal Douglas-fir. Wood Fiber Sci. 26:229–236.

Yang KC (1994).Impact of spacing on width and basal area of juvenile and mature wood in *Piceamariana* and *Piceaglauca*. Wood Fiber Sci. 26:479–488.

Zobel BJ, Buijtenen JP (1989). Wood variation its cause and control. Springer, Berlin Heidelberg New York.

Zobel BJ, Sprague JR (1998).Juvenile wood in forest trees.Springer, Berlin Heidelberg New York.

Zobel BJ, Webb C, Henson F (1959).Core or juvenile wood of loblolly pine and slash pine.Tappi 42(5):345–355.